Feedback Control of a Lower Limb Exoskeleton System by Determining Optimal LQR Weighting Matrices using Evolutionary Multi-objective Optimization*

1st Jatin Gupta
Department of Mechanical Engineering,
Indian Institute of Technology Kanpur
Kanpur, PIN: 208016, INDIA
Email: jgupta@iitk.ac.in

2nd Rituparna Datta
Department of Computer Science
University of South Alabama
Mobile, AL 36688, USA
Email: rdatta@southalabama.edu

3rd Arun Kumar Sharma
Department of Mechanical Engineering,
Indian Institute of Technology Kanpur
Kanpur, PIN: 208016, INDIA
Email: sarun@iitk.ac.in

4th Aviv Segev
Department of Computer Science
University of South Alabama
Mobile, AL 36688, USA
Email: segev@southalabama.edu

5th Bishakh Bhattacharya
Department of Mechanical Engineering,
Indian Institute of Technology Kanpur
Kanpur, PIN: 208016, INDIA
Email: bishakh@iitk.ac.in

***Abstract*—The present work discusses optimal feedback control of a lower limb exoskeleton by determining optimal Linear Quadratic Regulator (LQR) weighting matrices. A simplified model of human gait having four degrees of freedom is developed to describe the dynamics of the Single Support Phase (SSP) of the gait cycle. The system is linearized about the reference trajectory to apply an optimal controller. It is observed that the choice of weight matrices are important to controller performance. Instead of conventional diagonal weight matrices, the more complex symmetric weight matrix is used in the study. An optimization problem is formulated to find the optimal weighting matrix by minimizing tracking error of joint angles. Non-dominated sorting genetic algorithm (NSGA)-II is then used to obtain the solution of a multi-objective constrained optimization problem.**

***Index Terms*—exoskeleton, linear quadratic regulator, human gait, Evolutionary Computation, Multi-objective optimization, NSGA-II, design of experiment**

I. Introduction

With the aging process, many people start suffering from the problem of weak limbs resulting in mobility disorders and loss of sensory and motor function of limbs. Wearable robotic devices are viable solutions to help people suffering from these issues by augmenting their strength. These robotic devices, popularly known as exoskeletons, aid user by providing external power and controlling the dynamics to achieve desired motion. Due to the highly complex nature of human walking, designing an efficient wearable robotic device is a challenging process. There is a void for focused research to be carried out on enhancing the efficiency and cost reduction of the system. Mechanical design, actuators, and control strategy are the critical aspects of performance of exoskeletons[1].

In-depth research has been carried out to develop simplified yet realistic models of human gait. Vukobratović et al.[2] introduced the concept of Zero Moment Point (ZMP). This concept is widely used for stability and gait generation in biped robots. Kajita et al.[3] modeled human gait as the motion of inverted pendulum which laid the foundations for much other further research. Li and Todorov proposed Iterative Linear Quadratic Regulator (iLQR) approach to solve non-linear biological systems[4]. Park et al.[5] used a multi-objective evolutionary algorithm to generate an optimal trajectory of humanoid robots by employing a multi-objective quantum-inspired evolutionary algorithm to obtain solutions of weighting matrices in an iLQR method.

This study aims to design an optimal Linear Quadratic Regulator (LQR) controller for the exoskeleton system to minimize the feedback error and ensure the stability of the control system at each interval of time. The current paper is organized as follows. It begins with a discussion about the significant research work that has been carried out in recent years in the field of human biped modeling and control strategies. Next, a simplified dynamic model of the human bipedal gait, having four degrees of freedom has been presented. This is followed by designing an optimal Linear Quadratic Controller (LQR) for the linearized dynamics of the system, and closed loop system responses have been described. Since the performance of the LQR controller depends upon the choice of a weight matrix. Hence, an optimization problem is formulated then to determine weight matrix which minimizes

Seamless Affordable Assistive Technology for Health (SAATH) project sponsored by Department of Biotechnology (DBT) under the Ministry of Science and Technology, Government of India.

the total error of this trajectory follower problem. Finally, the conclusions are inferred, and possible future work that can be carried out has been suggested.

II. Dynamic Model of Human Gait

Broadly, human gait is comprised of two different phases as a whole - Double Support Phase and Single Support Phase. Double support phase (DSP) is the phase when both the legs are in contact with the ground, and human adjusts its posture for the next walking step; while, when only one leg is in contact with the ground, gait is said to be in the Single Support Phase (SSP). For an average human gait, roughly around 30% of the gait cycle is constituted with the double support phase, and the rest of the 70% is constituted with the single support phase [6]. Each leg undergoes a periodic motion for about 60% of the gait cycle acting as a supporting limb for the body (or in the stance phase). For the remaining 40% of the gait cycle, the leg performs a swing motion about the pelvis to propel the body forward while taking the forward step. The human bipedal locomotion can also be divided into motions in three perpendicular planes viz. *Sagittal plane*, the *Coronal or Frontal plane*, and the *Transverse Plane*.

As dynamic effects in frontal and transverse planes are comparatively small as compared to that of the sagittal plane, only sagittal plane modeling of human gait is considered for this work [7]. As the time during DSP is quite small compared to SSP, it can be assumed that model instantly starts another SSP after completing the previous one [8], and only single support phase modeling has been considered in the present work. Since the angular variation of the knee during stance phase is quite small [9], the motion of each leg in its stance phase can be modeled as the motion of an inverted pendulum; while the motion in the swing phase can be modeled as the motion of a triple pendulum. Figure 1 shows the simplified model of human gait.

The primary objective of any wearable robotic device is to assist the user and follow the motion trajectory and not hamper the movements. In this regard, one of the simplest cases of exoskeleton model will be having its joints perfectly aligned with the human body. In such a case, a combined human and exoskeleton system will have the same dynamics, and it can be treated as one single system. It is assumed that enough friction is present so that slipping does not occur and thus the stance leg can be considered to be fixed to the ground. For the sagittal plane motion, the hip joint is nearly in-line with the center of mass (COM) of the body. Thus the pivot point for the triple pendulum can be approximately taken at the same location as that of the COM.

Such a system has four degrees of freedom viz. Stance leg angle (ϕ), a Hip joint of swing leg (θ_1), Knee joint of swing leg (θ_2), and Ankle joint of swing leg (θ_A). Kinematic model of the system is derived using the forward kinematic approach. Ankle joint of stance leg, which is fixed to the ground is taken as the origin of the global coordinate system. Position vectors of COM of each link with respect to global coordinates are shown from (1) to (7). Here, r_i^O denotes

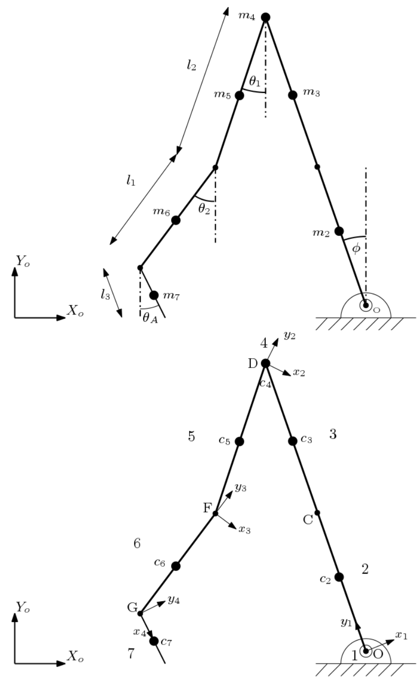

Fig. 1: Kinematic Model

coordinates of i concerning O (Origin at the ankle of stance leg) in the global coordinate reference frame.

$$r_{c1}^o = [0, 0, 0]^T \tag{1}$$

$$r_{c2}^o = R_1^o \, [0, \ l_1/2 \ , 0]^T \tag{2}$$

$$r_{c3}^o = R_1^o \, [0, \ l_1 + l_1/2 \ , 0]^T \tag{3}$$

$$r_{c4}^o = R_1^o \, [0, \ l_1 + l_2 \ , 0]^T \tag{4}$$

$$r_{c5}^o = r_{c4}^o + R_1^o R_2^1 \, [0, \ -l_2/2 \ , 0]^T \tag{5}$$

$$r_{c6}^o = r_F^o + R_1^o R_2^1 R_3^2 \, [0, \ -l_1/2 \ , 0]^T \tag{6}$$

$$r_{c7}^o = r_G^o + R_1^o R_2^1 R_3^2 R_4^3 \, [l_3/2 \ , 0, 0]^T \tag{7}$$

R_1^o, R_2^1, R_3^2, and R_4^3 are transformation matrices which are shown in (8) to (11), where R_j^i denotes transformation matrix from j^{th} reference frame to i^{th} reference frame.

$$R_1^o = \begin{bmatrix} cos(\phi) & -sin(\phi) & 0 \\ sin(\phi) & cos(\phi) & 0 \\ 0 & 0 & 1 \end{bmatrix} \tag{8}$$

$$R_2^1 = \begin{bmatrix} cos(\theta_1 - \phi) & -sin(\theta_1 - \phi) & 0 \\ sin(\theta_1 - \phi) & cos(\theta_1 - \phi) & 0 \\ 0 & 0 & 1 \end{bmatrix} \tag{9}$$

$$R_3^2 = \begin{bmatrix} cos(\theta_2 - \theta_1) & -sin(\theta_2 - \theta_1) & 0 \\ sin(\theta_2 - \theta_1) & cos(\theta_2 - \theta_1) & 0 \\ 0 & 0 & 1 \end{bmatrix} \tag{10}$$

$$R_4^3 = \begin{bmatrix} sin(\theta_A - \theta_2) & cos(\theta_A - \theta_2) & 0 \\ -cos(\theta_A - \theta_2) & sin(\theta_A - \theta_2) & 0 \\ 0 & 0 & 1 \end{bmatrix} \tag{11}$$

The governing dynamic equation for the system can be derived by defining the Lagrangian of the system. The kinetic energy of each rigid limb can be written as the sum of its translational and rotational kinetic energies.

$$T_i = \frac{1}{2} m_i V_{c_i}^T V_{c_i} + \frac{1}{2} \omega_{c_i}^T I_{c_i} \omega_{c_i} \tag{12}$$

Where, V_{c_i}, ω_{c_i}, and I_{c_i} are the velocity of center of mass, angular velocity and moment of inertia relative to center of mass respectively in global coordinate reference frame. Then, the equations of motion for the system can be written as:

$$\frac{d}{dt}\left(\frac{\partial \mathcal{L}}{\partial \dot{q}_i}\right) - \frac{\partial \mathcal{L}}{\partial q_i} + \frac{\partial \mathcal{P}}{\partial \dot{q}_i} = \ll_i \tag{13}$$

where, $\mathcal{L} = KE - PE$ is the Lagrangian of the system, $\mathbf{q} = [\phi, \theta_1, \theta_2, \theta_A]^T$ are the generalized coordinates, $\ll_i$ is the corresponding external torque acting on the system, and $\mathcal{R}_i = -\frac{\partial \mathcal{P}}{\partial \dot{q}_i}$ is the dissipative force present at the joint q_i. As the system has low velocity, linear damping of the form $\mathcal{R}_i = -c_i \dot{q}_i$ is considered, where c_i is the damping coefficient.

Solving (13) results in the system of 2^{nd} order non-linear differential equations which can be expressed in matrix notation as:

$$\begin{aligned} \o &= \mathbf{H}(\mathbf{q})\ddot{\mathbf{q}} + \mathbf{C}(\dot{\mathbf{q}}, \mathbf{q})\dot{\mathbf{q}} + \mathbf{G}(\mathbf{q}) \\ or, \quad \o &= \mathcal{H}(\mathbf{q})\ddot{\mathbf{q}} + \mathcal{G}(\dot{\mathbf{q}}, \mathbf{q}) \end{aligned} \tag{14}$$

where $\mathbf{H}$ corresponds to inertia term, $\mathbf{C}$ is the Coriolis component, and $\mathbf{G}$ is body force term.

III. Feedback Control

The problem of designing the control law for an exoskeleton system can be described as the trajectory follower problem. The system should follow the reference trajectory of human walking to assist the user. Reference trajectory for each degree of freedom in the model is generated using ADAMS based human body simulator LifeMOD, developed by Lifemodeler Incorporated, U.S.A. Human body model named "Casey" is selected as the reference model for gait analysis. The physical details of the model are listed in Table I.

TABLE I: Physical Details of the "Casey" model

Mass of Thigh	10.5 kg
Mass of Shin	2.8 kg
Mass of foot	1 kg
Mass of Upper Body	43 kg
Total Weight	71 kg
Length of Thigh	0.45 m
Length of Shin	0.45 m
Length of foot	0.15 m
Total Height	1.70 m

A. Linearization of system model

System equations in (14) are non-linear in nature and must be linearized before applying linear controller. Defining the state variable as $\mathbf{x} = [\mathbf{q}^T, \dot{\mathbf{q}}^T]^T$ and rearranging the terms results in state space form as shown in (15).

$$\begin{aligned} \dot{\mathbf{x}} &= \begin{bmatrix} \dot{\mathbf{q}} \\ \mathcal{H}(\mathbf{q})^{-1}(\o - \mathcal{G}(\dot{\mathbf{q}}, \mathbf{q})) \end{bmatrix} \\ or, \quad \dot{\mathbf{x}} &= f(\mathbf{x}, \mathbf{u}) \end{aligned} \tag{15}$$

It can be linearized about the operating point using Taylor series. Let $(\mathbf{x_0(t)}, \mathbf{u_0(t)})$ be a generalized point on reference trajectory, then defining $(\bar{\mathbf{x}}(\mathbf{t}), \bar{\mathbf{u}}(\mathbf{t})) = (\mathbf{x(t)} - \mathbf{x_0(t)}, \mathbf{u(t)} - \mathbf{u_0(t)})$ as error variable, linearized system can be written as [10]:

$$\begin{aligned} \dot{\bar{\mathbf{x}}}(t) &= \mathbf{A}(t)\bar{\mathbf{x}}(t) + \mathbf{B}(t)\bar{\mathbf{u}}(t) \\ where, \quad \mathbf{A} &= \begin{bmatrix} \mathbf{0} & \mathbf{I} \\ \mathcal{H}^{-1}[\frac{\partial \mathcal{H}}{\partial \mathbf{x}}\mathcal{H}^{-1}(\mathcal{G} - \o) - \frac{\partial \mathcal{H}}{\partial \mathbf{x}}] \end{bmatrix} \\ and, \quad \mathbf{B} &= \begin{bmatrix} \mathbf{0} \\ \mathcal{H}^{-1} \end{bmatrix} \end{aligned} \tag{16}$$

At a particular instant of time, (16) shows a linear relationship between $\dot{\bar{\mathbf{x}}}$ and $(\bar{\mathbf{x}}, \bar{\mathbf{u}})$ with constant coefficients. As the system is highly unstable, it is required to design an optimal feedback controller for the system which guarantees the stability of the closed-loop system. Linear Quadratic Regulator(LQR) is a well known optimal controller for a linear system. Hence, LQR based feedback control is applied to the system.

B. LQR Control

As the reference point, itself is time-varying, gain scheduling approach is used which uses a family of linear controllers around different operating points. For implementing the linear optimal controller, LQR, a cost function J is defined such that minimizing the cost function results in trajectory stabilization.

$$J = \frac{1}{2}\int_0^\infty [\bar{\mathbf{x}}(t)^T \mathbf{Q}\ \bar{\mathbf{x}}(t) + \bar{\mathbf{u}}(t)^T \mathbf{R}\ \bar{\mathbf{u}}(t)]dt \tag{17}$$

$\mathbf{Q}$ and $\mathbf{R}$ are weighting factors associated with state cost and input cost respectively. $\mathbf{Q}$ should be a positive semidefinite

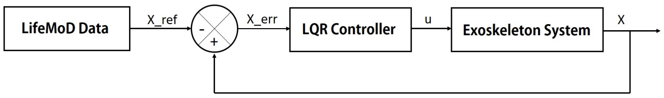

Fig. 2: Control flow of the system

and $\mathbf{R}$ should be a positive definite matrix. Feedback control law which minimizes (17) is given by

$$\begin{aligned} \bar{\mathbf{u}}(t) &= -\mathbf{K}(t)\bar{\mathbf{x}}(t) \\ where, \quad \mathbf{K}(t) &= \mathbf{R}^{-1}\mathbf{B}(t)^T\mathbf{S}(t)\bar{\mathbf{x}}(t) \end{aligned} \tag{18}$$

$\mathbf{S}$ is the solution of Algebraic Riccati Differential Equation. The control flow diagram is shown in figure 2.

Taking both $\mathbf{Q}$ and $\mathbf{R}$ as identity matrices, closed loop results are shown in figure 3.

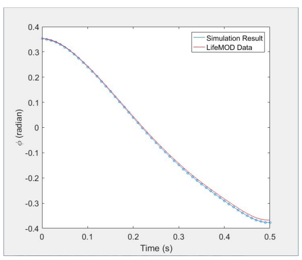

(a) Stance Leg

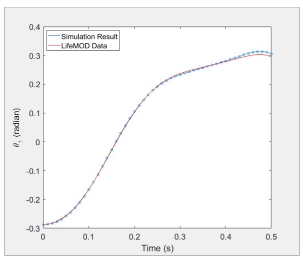

(b) Hip Joint of Swing Leg

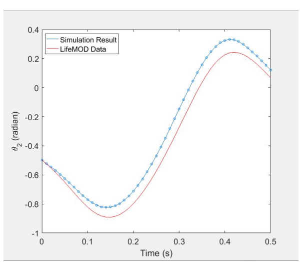

(c) Knee Joint of Swing Leg

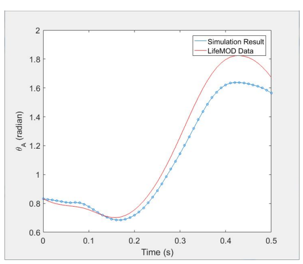

(d) Ankle Joint of Swing Leg

Fig. 3: Angular Displacement after feedback control

The normalized RMS error for ϕ, θ_1, θ_2, and θ_A are 0.79%, 0.66%, 7.38%, and 11.44%. Although the system is stabilized, but at some points non-linearity of the system is very large for the linear controller. It shows that the controller with identity weight matrix in the present case is not robust enough and the controller requires a different weight matrix.

IV. Optimal Weighting Matrices

Results of the closed-loop system show that instead of penalizing each variable equally by taking an identity matrix, the controller requires different weighting factor for each variable. Generally, $\mathbf{Q}$ is taken as Identity matrix and $\mathbf{R}$ is varied by trial and error. In the present work, an optimization problem is formulated to determine the optimal $\mathbf{R}$ matrix to minimize Root Mean Square error of each degree of freedom simultaneously.

For the optimization problem, mathematical relations between matrix elements and normalized RMS error of angular displacements are the objective functions which are to be minimized. As no direct mathematical relationship is present, a regression model is used to obtain the approximate functions.

A. *Design of Experiment*

Design of experiments (DOE) has been used to study the effect of independent variables on the output in a controlled experiment. It involves identifying the independent variables that affect the experiment and then examining their effects on a dependent variable or response. The tests are performed using the Box−Behnken (BB) design of response surface methodology (RSM) as it carries out 'non-sequential experiments with fewer design points' [11]. The BB design needs only three levels for an experiment since no points lie at the vertices of the experiment region. Thus, it assists in the better estimation of the first and second-order coefficients even with fewer design points. Thus for the same number of factors, BB design can be less expensive than central composite design (CCD), and it has also been proven useful if the safe operating zone is known for the process. For analyzing the experimental data, Design Expert 10.0 software is used. It estimates a suitable mathematical relationship between input and output parameters using regression analysis.

Generally, a second-order model is employed in response surface methodology of a form as shown in equation 19.

$$y = \beta_0 + \beta_1 a_1 + \beta_2 a_2 + \beta_{12} a_1 a_2 + \beta_{11} a_1^2 + \beta_{22} a_2^2 + \epsilon \tag{19}$$

where, y is the output variable, (a_1, a_2) are the input parameters, (a_1^2, a_2^2) and $(a_1 a_2)$ are the square and interaction terms of parameters respectively. β's are the unknown regression coefficients and ϵ is the error.

$$\mathbf{R} = \begin{bmatrix} x_1 & x_2 & x_3 & x_4 \\ x_2 & x_5 & x_6 & x_7 \\ x_3 & x_6 & x_8 & x_9 \\ x_4 & x_7 & x_9 & x_{10} \end{bmatrix} \tag{20}$$

For the optimization problem, $\mathbf{R}$ is taken as a symmetric matrix having four diagonal and six off-diagonal independent variables $(x_1, x_2, ..., x_{10})$. Normalized RMS error for each joint angle are the dependent variables. Simulations are performed to examine the effect of the matrix in 20 on the output. For designing the experiment, to ensure positive definiteness of the matrix, diagonal elements are given low and high values 5 and 10 respectively, and off-diagonal elements are given low and high values 0 and 2 respectively. The experimental data collected according to BoxBehnken design are analyzed to establish the relation between independent input parameters and the responses using analysis of variance (ANOVA). It is observed that RMS error for ϕ does not vary much and is always $< 1\%$. Thus, RMS errors for θ_1, θ_2, and θ_A are taken as three objective functions for the multi-objective optimization problem. The coefficient of determination (R^2) and adjusted R^2 values are 0.9756 and 0.9668 for R1, 0.9995 and 0.9993 for R2, and 0.9987 and 0.9983 for R3 respectively.

B. Genetic Algorithm

For the optimization problem, elements of matrix in (20) are taken as independent parameters which are to be optimized. The requirement on $\mathbf{R}$ is that it should be a positive definite matrix. Thus following constraints are defined for the problem:

$$\begin{aligned} x_1 &> 0 \\ \begin{vmatrix} x_1 & x_2 \\ x_2 & x_5 \end{vmatrix} &> 0 \\ \begin{vmatrix} x_1 & x_2 & x_3 \\ x_2 & x_5 & x_6 \\ x_3 & x_6 & x_8 \end{vmatrix} &> 0 \\ det(\mathbf{R}) &> 0 \end{aligned} \tag{21}$$

Variable bounds are defined in (22).

$$\begin{aligned} 0.001 \leq x_1 &\leq 10 \\ 0 \leq x_2 &\leq 10 \\ 0 \leq x_3 &\leq 10 \\ 0 \leq x_4 &\leq 10 \\ 0.001 \leq x_5 &\leq 10 \\ 0 \leq x_6 &\leq 10 \\ 0 \leq x_7 &\leq 10 \\ 0.001 \leq x_8 &\leq 10 \\ 0 \leq x_9 &\leq 10 \\ 0.001 \leq x_{10} &\leq 10 \end{aligned} \tag{22}$$

The formulation shows that the objective function is nonlinear. As a result, evolutionary multi-objective function technique is used for optimization. Non-dominated sorting genetic algorithm-II (NSGA-II) [12] technique is used for optimization of the objective functions and to obtain the optimal values of the variables $(x_1, x_2, ..., x_{10})$. The non-dominated solution between R1, R2, and R3 is shown in figure 4.The parameters for NSGA-II are as follows:

Population size = 200,
Number of generations = 500,
Crossover probability (Simulated Binary Crossover) = 0.9,
SBX index = 10,
Mutation (Polynomial mutation) probability = 1/number of variables,
Mutation index = 50

Figure 4 shows the Pareto optimal solution for the three objective functions. It can be observed that the objective functions are conflicting to each other as at the minimum point of one error; the other corresponding error gets maximized. Table II shows the values of objective functions with corresponding variable values.

$$\mathbf{R} = \begin{bmatrix} 0.506 & 0.002 & 1.441 & 1.692 \\ 0.002 & 0.22 & 0.004 & 0.099 \\ 1.441 & 0.004 & 9.999 & 2.769 \\ 1.692 & 0.099 & 2.769 & 9.272 \end{bmatrix} \tag{23}$$

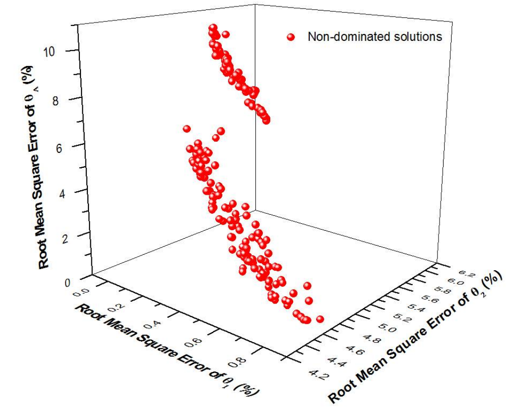

Fig. 4: Non-dominated solutions

One random set of optimal values are taken from Table II (6^{th} column of data) and the system is simulated. $\mathbf{R}$ matrix is shown in (23) and system responses in figure 5. Normalized RMS error obtained for ϕ, θ_1, θ_2, and θ_A are 0.7%, 1.17%, 2.98%, and 2.92% respectively. It is observed that the system error responses from the computation and those obtained from optimization are close to each other. An explanation for the difference in the results is that the relation between input and output parameters are obtained from the regression analysis and the estimated model does not necessarily fit sampled data exactly. The model can be improved with further research to get more accurate results.

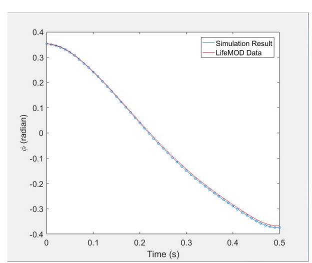

(a) Stance Leg

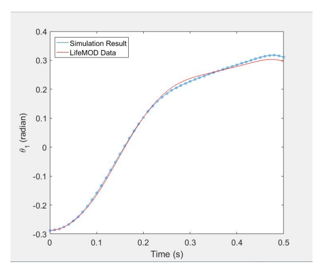

(b) Hip Joint of Swing Leg

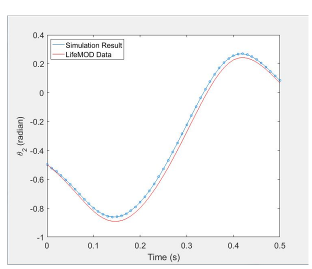

(c) Knee Joint of Swing Leg

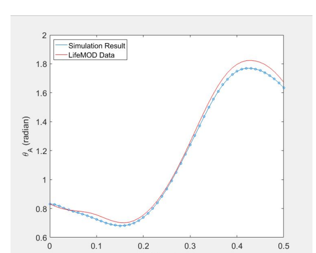

(d) Ankle Joint of Swing Leg

Fig. 5: Angular Displacement after feedback control using optimal value of R

V. Conclusion

In the present work, a simplified model of human gait has been developed using mathematical models of inverted and triple pendulums. Reference trajectory for each degree of

TABLE II: Objective function and parameter values

R1	0.555	0.802	0.764	0.355	0.105	0.54	0.429	0.019	0.434	0.241	0.021
R2	4.335	4.638	4.653	4.721	5.016	4.631	4.793	5.563	4.821	4.775	5.545
R3	7.611	0.178	0.252	4.074	5.486	1.841	2.606	8.206	0.840	5.036	8.164
$\mathbf{x_1}$	0.445	0.362	0.355	0.106	0.124	0.506	0.079	5.344	0.296	0.109	5.344
$\mathbf{x_2}$	0.001	0.000	0.000	0.000	0.000	0.002	0.001	0.018	0.000	0.001	0.003
$\mathbf{x_3}$	1.021	1.548	1.548	0.604	0.569	1.441	0.637	3.456	1.561	0.450	3.335
$\mathbf{x_4}$	1.943	1.127	1.119	0.560	0.040	1.692	0.208	7.068	0.672	0.554	7.143
$\mathbf{x_5}$	9.927	0.134	0.133	1.811	1.195	0.220	0.760	0.056	0.039	1.793	0.005
$\mathbf{x_6}$	1.741	0.283	0.141	0.084	0.002	0.004	0.019	0.001	0.086	0.019	0.001
$\mathbf{x_7}$	0.026	0.036	0.034	1.883	2.182	0.099	1.673	0.003	0.043	2.406	0.003
$\mathbf{x_8}$	9.992	9.995	9.967	9.986	9.997	9.999	9.998	9.999	9.874	9.991	9.890
$\mathbf{x_9}$	1.291	1.725	1.814	2.705	3.863	2.769	2.778	3.027	2.743	3.246	2.757
$\mathbf{x_{10}}$	9.968	9.488	9.492	9.798	6.047	9.272	9.714	9.759	6.423	9.973	9.969

freedom was generated using LifeMOD. Optimal feedback controller (LQR) has been used after linearizing the system about reference trajectory. It was observed that appropriate selection of weight matrix in the cost function is vital in minimizing the error for a trajectory follower problem. For determining optimal weight matrix, an optimization problem is formulated to minimize the root mean square error of the system variables. Weight matrix $\mathbf{R}$ was taken as a symmetric matrix having 10 independent elements which are to be optimized. It has been observed that the objective functions are conflicting. R1 is conflicting with both R2 and R3, but R2 and R3 are not conflicting with each other. As no direct mathematical relation was present between weight matrix elements and system error, a 2^{nd} order polynomial relation was developed using regression analysis which can account for small error in computed and optimization data. Nevertheless, the optimal solution shows quite good results for trajectory follower problem.

The future work can be extended by formulating a more realistic mathematical model considering external disturbance and contact constraints. The triple pendulum model as considered in this work will play a crucial role as foot will be subjected to ground reactions and for zero moment point (ZMP) stability in 3-D motion. Since, the walking pattern of each user differs slightly, hence instead of an optimal controller, an adaptive optimal controller can be applied. Also, the regression model for weight matrix optimization can be improved to obtain more accurate optimization results.

ACKNOWLEDGMENT

The authors acknowledge the support of this research under Seamless Affordable Assistive Technology for Health (SAATH) project sponsored by Department of Biotechnology (DBT) under the Ministry of Science and Technology, Government of India.

VI. SUPPLEMENTARY MATERIAL

A. Kinetic and Potential energy of the system

The Lagrangian of the system $\mathcal{L} = KE - PE$ requires mathematical expression of kinetic and potential energies of the system. The kinetic energies for individual links are shown here, where corresponding link numbers are shown in figure 1.

$$KE_1 = 0 \tag{24}$$

$$KE_2 = \frac{m_2}{24}\left(b^2 + 4{l_1}^2\right)\dot{\phi}^2 \tag{25}$$

$$KE_3 = \frac{m_3}{24}\left(b^2 + 12{l_1}^2 + 12 l_1 l_2 + 4{l_2}^2\right)\dot{\phi}^2 \tag{26}$$

$$KE_4 = \frac{m_4}{2}\left(l_1 + l_2\right)^2\,\dot{\phi}^2 \tag{27}$$

$$\begin{aligned} KE_5 = \frac{m_5}{8}\Big(2\,l_1\,\cos(\phi)\,\dot{\phi} + 2\,l_2\,\cos(\phi)\,\dot{\phi} - l_2\,\cos(\theta_1)\,\dot{\theta_1}\Big)^2 \\ + \frac{m_5}{8}\Big(2\,l_1\,\sin(\phi)\,\dot{\phi} + 2\,l_2\,\sin(\phi)\,\dot{\phi} - l_2\,\sin(\theta_1)\,\dot{\theta_1}\Big)^2 \\ + \frac{m_5}{24}\left(b^2 + {l_2}^2\right)\dot{\theta_1}^2 \end{aligned} \tag{28}$$

$$\begin{aligned} KE_6 = \frac{m_6}{8}\Big((l_1\,\cos(\theta_2)\,\dot{\theta_2} - 2\,l_1\,\cos(\phi)\,\dot{\phi} - 2\,l_2\,\cos(\phi)\,\dot{\phi} \\ + 2\,l_2\,\cos(\theta_1)\,\dot{\theta_1}))^2 + \frac{m_6}{8}\Big((l_1\,\sin(\theta_2)\,\dot{\theta_2} - 2\,l_1\,\sin(\phi)\,\dot{\phi} \\ - 2\,l_2\,\sin(\phi)\,\dot{\phi} + 2\,l_2\,\sin(\theta_1)\,\dot{\theta_1}))^2 + \frac{m_6}{24}\left(b^2 + {l_1}^2\right)\dot{\theta_2}^2 \end{aligned} \tag{29}$$

$$\begin{aligned} KE_7 = \frac{m_7}{8}\Big(l_3\,\cos(\theta_A)\,\dot{\theta_A} + 2\,l_1\,\cos(\theta_2)\,\dot{\theta_2} + 2\,l_2\,\cos(\theta_1)\,\dot{\theta_1} \\ - 2\,l_1\,\cos(\phi)\,\dot{\phi} - 2\,l_2\,\cos(\phi)\,\dot{\phi}\Big)^2 + \frac{m_7}{8}\Big(l_3\,\sin(\theta_A)\,\dot{\theta_A} \\ + 2\,l_1\,\sin(\theta_2)\,\dot{\theta_2} + 2\,l_2\,\sin(\theta_1)\,\dot{\theta_1} - 2\,l_1\,\sin(\phi)\,\dot{\phi} \\ - 2\,l_2\,\sin(\phi)\,\dot{\phi}\Big)^2 + \frac{m_7}{24}\left(h^2 + {l_3}^2\right)\dot{\theta_A}^2 \end{aligned} \tag{30}$$

And the potential energies for individual links.

$$PE_1 = 0 \tag{31}$$

$$PE_2 = (g\,l_1\,m_2\cos(\phi))/2 \tag{32}$$

$$PE_3 = g\,m_3\cos(\phi)\,\left(l_1 + l_2/2\right) \tag{33}$$

$$PE_4 = g\,m_4\cos(\phi)\,\left(l_1 + l_2\right) \tag{34}$$

$$PE_5 = -g\,m_5\left((l_2\cos(\theta_1))/2 - \cos(\phi)\,\left(l_1 + l_2\right)\right) \tag{35}$$

$$\begin{aligned} PE_6 = -g\,m_6(l_2\cos(\theta_1) - \cos(\phi)\,\left(l_1 + l_2\right) \\ + (l_1\cos(\theta_2))/2) \end{aligned} \tag{36}$$

$$\begin{aligned} PE_7 = -g\,m_7(l_2\cos(\theta_1) - \cos(\phi)\,\left(l_1 + l_2\right) + l_1\cos(\theta_2) \\ - (l_3\cos(\theta_A))/2) \end{aligned} \tag{37}$$

B. Objective Functions

The mathematical relations for the three objective functions (R1, R2, and R3) are obtained through regression analysis. R1 corresponds to Normalized RMS error for θ_1, R2 for θ_2, and R3 for θ_A.

$$
\begin{aligned}
R1 = 0.716 + 0.024x_1 + 0.312x_2 - 0.065x_3 + 0.095x_4 \\
+0.087x_5 + 0.296x_6 - 0.106x_7 - 0.139x_8 + 0.14x_9 \\
-0.021x_{10} - 0.03x_1x_2 + 0.009x_1x_3 - 0.011x_1x_4 \\
-0.039x_2x_3 + 0.032x_2x_4 + 0.018x_2x_5 + 0.017x_2x_6 \\
-0.025x_2x_7 + 0.024x_2x_9 - 0.013x_2x_{10} - 0.022x_3x_4 \\
-0.01x_3x_5 + 0.016x_3x_7 + 0.011x_3x_8 - 0.020x_3x_9 \\
+0.011x_3x_{10} + 0.018x_4x_5 - 0.006x_4x_8 + 0.022x_4x_9 \\
-0.011x_4x_{10} - 0.01x_5x_6 - 0.014x_5x_8 + 0.026x_5x_9 \\
-0.011x_5x_{10} - 0.015x_6x_8 + 0.01x_7x_8 - 0.024x_7x_9 \\
-0.021x_8x_9 + 0.008x_8x_{10} - 0.02x_9x_{10} + 0.024x_2^2 \\
+0.008x_5^2 + 0.009x_8^2 + 0.024x_9^2 + 0.003x_{10}^2
\end{aligned}
\tag{38}
$$

$$
\begin{aligned}
R2 = 7.354 + 0.426x_1 + 0.097x_2 - 0.009x_3 - 0.272x_4 \\
-0.003x_5 - 0.04x_6 + 0.007x_7 - 0.335x_8 - 0.049x_9 \\
-0.037x_{10} + 0.009x_1x_2 + 0.009x_1x_3 + 0.014x_1x_4 \\
+0.001x_1x_5 - 0.004x_1x_7 + 0.003x_1x_8 - 0.005x_1x_9 \\
+0.001x_1x_{10} - 0.007x_2x_5 + 0.016x_2x_7 - 0.003x_2x_8 \\
+0.005x_2x_9 + 0.01x_3x_4 - 0.004x_3x_5 - 0.015x_3x_6 \\
-0.004x_3x_8 - 0.004x_3x_{10} - 0.003x_4x_8 + 0.009x_4x_{10} \\
+0.004x_5x_9 - 0.001x_5x_{10} + 0.006x_6x_7 - 0.003x_6x_8 \\
-0.007x_6x_9 - 0.006x_8x_9 - 0.002x_8x_{10} + 0.003x_9x_{10} \\
-0.019x_1^2 - 0.024x_2^2 + 0.014x_3^2 - 0.01x_4^2 + 0.024x_6^2 \\
+0.013x_8^2 + 0.022x_9^2 + 0.002x_{10}^2
\end{aligned}
\tag{39}
$$

$$
\begin{aligned}
R3 = 14.893 + 0.973x_1 + 2.919x_2 - 1.124x_3 + 1.03x_4 \\
+1.615x_5 - 0.358x_6 + 0.588x_7 - 1.463x_8 + 1.607x_9 \\
-1.485x_{10} - 0.092x_1x_2 + 0.089x_1x_3 - 0.071x_1x_4 \\
+0.075x_1x_5 + 0.022x_1x_7 - 0.016x_1x_8 + 0.018x_1x_9 \\
-0.021x_1x_{10} - 0.029x_2x_5 + 0.048x_2x_6 - 0.05x_2x_7 \\
-0.066x_2x_{10} - 0.054x_3x_4 - 0.143x_3x_6 + 0.073x_3x_7 \\
+0.11x_4x_6 - 0.08x_4x_7 - 0.015x_4x_8 - 0.056x_5x_7 \\
-0.035x_5x_{10} + 0.045x_6x_8 - 0.024x_6x_{10} - 0.015x_7x_8 \\
-0.11x_8x_9 + 0.057x_8x_{10} - 0.065x_9x_{10} - 0.049x_1^2 \\
-0.073x_2^2 + 0.092x_4^2 - 0.068x_5^2 + 0.084x_7^2 + 0.033x_8^2 \\
+0.162x_9^2 + 0.059x_{10}^2
\end{aligned}
\tag{40}
$$

References

[1] B. Chen, H. Ma, L.-Y. Qin, F. Gao, K.-M. Chan, S.-W. Law, L. Qin, and W.-H. Liao, "Recent developments and challenges of lower extremity exoskeletons," *Journal of Orthopaedic Translation*, vol. 5, pp. 26–37, April 2016.

[2] M. Vukobratović and B. Borovac, "Zero-moment pointthirty five years of its life," *International Journal of Humanoid Robotics*, vol. 1, no. 01, pp. 157–173, 2004.

[3] S. Kajita and K. Tani, "Study of dynamic biped locomotion on rugged terrain-derivation and application of the linear inverted pendulum mode," in *Robotics and Automation, 1991. Proceedings., 1991 IEEE International Conference on*. IEEE, 1991, pp. 1405–1411.

[4] W. Li and E. Todorov, "Iterative linear quadratic regulator design for nonlinear biological movement systems." in *ICINCO (1)*, 2004, pp. 222–229.

[5] I.-W. Park, K.-B. Lee, and J.-H. Kim, "Multi-objective evolutionary algorithm-based optimal posture control of humanoid robots," in *Evolutionary Computation (CEC), 2012 IEEE Congress on*. IEEE, 2012, pp. 1–7.

[6] M. Kitagawa, "University of Texas at Dallas, notes on walking," http://www.utdallas.edu/atec/midori/Handouts/walkingGraphs.htm, accessed: 2017-05-10.

[7] T. McGeer, "Passive dynamic walking," *The International Journal of Robotics Research*, vol. 9, no. 2, pp. 62–82, April 1990.

[8] J.-S. Yang and A. Shahabuddin, "Trajectory planning and control for a five-degree-of-freedom biped locomotion system," in *Proceedings of the American Control Conference, 1994*, vol. 3. IEEE, 1994, pp. 3105–3109.

[9] S. Kajita, F. Kanehiro, K. Kaneko, K. Yokoi, and H. Hirukawa, "The 3d linear inverted pendulum mode: A simple modeling for a biped walking pattern generation," in *Intelligent Robots and Systems, 2001. Proceedings. 2001 IEEE/RSJ International Conference on*, vol. 1. IEEE, 2001, pp. 239–246.

[10] "Underactuated Robotics: Algorithms for Walking, Running, Swimming, Flying, and Manipulation (Course Notes for MIT 6.832)," 2014. [Online]. Available: http://people.csail.mit.edu/russt/underactuated/tocite.html

[11] C. P. Mohanty, S. S. Mahapatra, and M. R. Singh, "A particle swarm approach for multi-objective optimization of electrical discharge machining process," *Journal of Intelligent Manufacturing*, vol. 27, no. 6, pp. 1171–1190, December 2016.

[12] K. Deb, A. Pratap, S. Agarwal, and T. Meyarivan, "A fast and elitist multiobjective genetic algorithm: Nsga-ii," *Evolutionary Computation, IEEE Transactions on*, vol. 6, no. 2, pp. 182–197, 2002.